

# Ultimate Compressive Strain in Lightweight Aggregate Concrete Beams

Jelena Zivkovic<sup>1</sup>, Jan Arve Øverli<sup>1</sup>

<sup>1</sup>*Department of Structural Engineering, Norwegian University of Science and Technology (NTNU), Trondheim, Norway*

## Abstract

The major concern when using lightweight aggregate concrete (LWAC) in structural applications compared to normal weight concrete (NWC) is the more brittle post-peak behaviour and reduced ultimate strain, especially in compression. To investigate this six LWAC over-reinforced beams, with geometry 210-330x550x4500 mm, were subjected to four point bending with a constant moment zone of 1m between loading points. In this zone were varied main test parameters: the spacing of transverse reinforcement, amount of longitudinal compressive reinforcement and size of concrete cover. Strains were measured combining DIC, strain gauges and LVDTs. Five the tested beams showed ductile behaviour and ultimate compressive strain registered in the beams was in range 3.4-3.8%. This indicate that standards underestimate ultimate compressive strain in LWAC structures from 30-50%.

## 1. Introduction

Lightweight aggregate concrete (LWAC) has been used as a construction material from ancient times [1], with the main aim to reduce the dead weight of structures. Reduction of weight allows reduction of the structures dimensions, especially in seismic regions and areas with low bearing capacity. Handling and transport of precast elements from LWAC is easier and more economical. Until now, LWAC concrete is applied with great success in many advanced structures like bridges, offshore structures and skyscrapers [2]-[5]. Several different standards define LWAC as concrete with an oven dry density below 2000 kg/m<sup>3</sup> and with maximum strength about 80 MPa [6], [7]. Even with the major advantage of reduced weight and high strength-to-weight ratio compared to conventional concrete, the use of LWAC is still limited as a mainstream construction material. The main reason is the more brittle post-peak material behaviour that result with reduced ultimate compressive strain compared to normal density concrete (NWC). The brittleness of concrete is characterized by sensitivity to stress concentrations and a rapid crack/fracture development. For structural analysis, it is essential to know the complete stress-strain curve under uniaxial compression including the descending branch [8], [9]. The main emphasis in this work is on the post-peak strain-softening response, which is for LWAC steep and short since concrete behave in a brittle manner. An experimental program is conducted to investigate the post-peak behaviour of LWAC and ultimate strain in compression and bending. The program consist of six LWAC over-reinforced beams, subjected to four point bending. The geometry of the beams were 210-330 x 550 x 4500 mm (width x height x length). In addition, small samples cubes and cylinders were casted to decide the material quality. The test setup was designed to produce a constant moment zone of one meter between loading points. The main test parameters, varying in the constant compression zone, were the spacing of transverse reinforcement, amount of longitudinal compressive reinforcement and size of concrete cover. The ultimate capacity was evaluated by following the rules in Eurocode and the Norwegian code [6], [7] for design of concrete structures. All the tested beams failed in compression between the two loading points. Reinforcement detailing influenced the cracking of the compression zone in the beams. The beam without transversal reinforcement showed very explosive and brittle behaviour while all other beams showed ductile behaviour. The strain level in the concrete and reinforcement were measured with strain gauges (SG) and Linear Variable Differential Transformers (LVDT) at one side of the beam. On the other side, Digital Image Correlation (DIC) method was used [11], [12]. To produce the concrete, a lightweight aggregate argillite slate from North Carolina, called Stalite [13], was used to achieve an oven-dry density of about 1850 kg/m<sup>3</sup> and a compressive cylinder strength of about 65 MPa.

## 2. Experimental program and methodology

### 2.1 Test parameters

The experimental program include six over-reinforced LWAC beams which were subjected to a four point bending test, with a constant moment zone of one meter between the loading points. This type of experimental program was proposed in order to eliminate the effect of frictional restraint on post-ultimate deformation, what is typical for uniaxial compression tests [14]. This testing technique allow lateral expansion of the central zone in all directions and provide testing of the LWAC under multiaxial states of stress. Size of the compressive testing zone was approximately 300x1000 mm. The parameters varied in the beams were the stirrup spacing, amount of compressive reinforcement and size of concrete cover. All the beams were overreinforced to provide a compressive bending failure. Outside of the testing zone, all the beams had the same stirrups distribution designed to avoid shear failure. The moment and shear capacity of the beams has been calculated in accordance with Eurocode 2 and Norwegian code [6], [7]. The maximum compressive strain used in the calculation was  $\epsilon_{cu2}=2.52\%$ . Table 1 describe the test program.

Table 1 Test parameters

Beam No.	Beam Identification	Stirrup spacing -s [mm]	Concrete cover-c [mm]	Compressive reinforcement $A_c$	Capacity $P_{calc}$ [kN]
1	LWAC65_20_0	-	20	2 $\phi$ 12	729
2	LWAC65_20_200	200	20	2 $\phi$ 12	729
3	LWAC65_20_60	60	20	2 $\phi$ 12	729
4	LWAC65_20_100	100	20	2 $\phi$ 12	729
5	LWAC65_40_100	100	40	2 $\phi$ 12	726
6	LWAC65_40_200*	200	40	2 $\phi$ 25	800

#### 2.1.1 Test specimens

The beams measured (width x height x length) 210-330 x 550 x 4500 mm. All the beams were over-reinforced with ten  $\phi$ 20 mm bars in tension zone in order to provide compressive failure. Outside the constant bending zone stirrups  $\phi$ 10 mm were distributed along the shear spans on 70mm distance to avoid shear failure. In compressive zone, all beams 1-5 had two longitudinal bars  $\phi$ 16 mm and beam 6 two bars  $\phi$ 25 mm. Short longitudinal bar  $\phi$ 8 mm were set in testing compressive zone in all the tested beams as the carrier of the strain gauges. This bar was able to move together with concrete since it was not fixed at the edges. Stiff anchorage of tension reinforcement at the support was provided with a welding steel plate. Fig. 1 gives the beam geometry and cross section details between the loading points.

All the beams and small samples, cubes and cylinders, were cast from the same concrete batch. The beams were demoulded 24 hours after casting, and stored in the laboratory at approximately 20 °C under wet burlaps covered with a plastic sheet. They were uncovered two days before the test. Finally, the beams were painted white for easier detection of cracks and prepared for instrumentation. The test age of the beams varied from 37 to 59 days.

To establish the mechanical properties of the LWAC, cubes (with dimensions 100x100x100 mm), cylinders ( $\phi$ 100x200mm) and small beams (100x100x1200mm) were casted to find the stress-strain diagram, the compressive strength for cube and cylinder, the tensile strength, Young's module of elasticity, and the fracture energy. All these small specimens were demoulded after 24 hours and kept

in water until testing day. In order to follow material characteristics compression tests on cubes and cylinders were carried out continuously with the beam testing.

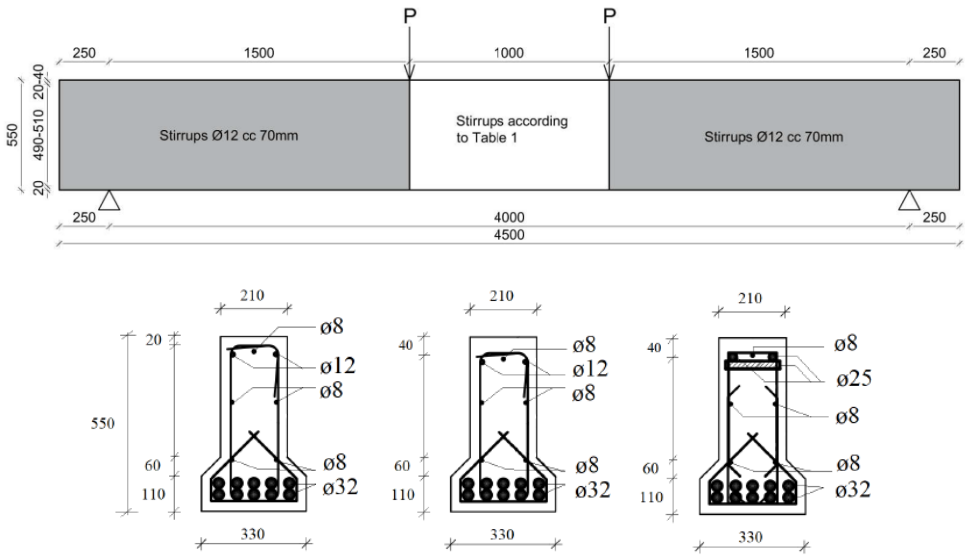


Fig. 1 Beam geometry and reinforcement layouts between the loading points. Dimensions are in [mm].

## 2.2 Material and mix properties

The concrete mixture was prepared from one batch at a concrete stationary plant and in a concrete truck mixer. Lightweight aggregate was first placed in a concrete truck and later mortar was added. Mixing and transport was done in a concrete truck mixer. The lightweight aggregate was  $\frac{1}{2}$ " fraction from Stalite [13]. The moisture content and the absorbed water in the Stalite were measured to be able to design the concrete mix [2]. The moisture content was 11.43%, and the absorption after 24 hours and 100 hours was 6.54% and 8.32%, respectively. Table 2 gives the concrete mixture. The mixing was done using combination of concrete stationary plant capacity 4 m<sup>3</sup> and concrete truck mixer 6 m<sup>3</sup> laboratory mixer. Mixing was done continuously in a truck mixer during a transport of 15 minutes. Characteristics of the fresh concrete were: density 2013 kg/m<sup>3</sup>, air content 2.4% and slump 230 mm. The reinforcement was of the type B500NC [15]. Assumed yielding stress of the reinforcement was 530 MPa.

Table 2 Concrete mix for LWAC 65

Constituent	Weight [kg/m <sup>3</sup> ]
Cement (Norcem Anlegg FA)	430.75
Silica fume (Elkem Microsilica)	22.38
Water (free+absorbed 24 hour)	123.33+55.17=178.5
Sand (Ramlo 0-8 mm)	595.31
Sand (Ramlo 0-2 mm)	249.65
Aggregate (Stalite $\frac{1}{2}$ " )	550
Superplasticizer (Mapei Dynamon SR-N)	5.4

### 2.3 Test Setup and procedure

Fig. 2 shows the experimental setup. The load was applied by mechanical screw jack and transferred to the test beam through a steel spreader beam. Two steel rollers supported the beam and covered the entire width of the beam. The loading point has free rotation transversal to the beam. Between jacks and the beam surface, it was used a 100 mm wide steel plates and a 15 mm thick fibreboard with the same width. The supports were both free for rotation and displacement in the longitudinal direction. At the supports, only steel plates were between the support and the beam. The supports were placed 250 mm from the beam-ends. To avoid anchorage problems, tension reinforcement bars were welded to the steel plate dimensions 30x60x330mm in this region. The load was measured by an electrical load cell under the screw jack with a maximum capacity 2000 kN. Three linear variable displacement transducers (LVDT), one at the mid-span and two above each loading point measured the deflections of the beam. Additional five LVDTs measured strain at the concrete surface. Three of them measured strains in the compressive zone and two strains in the tensile zone. The LVDTs were placed in the middle cross section and they measured deflection over a distance of 200 mm. In addition, six strain gauges (SG, type FLA-6-11-5L with gauge resistance of  $119.5 \pm 0.5 \Omega$ ) were inserted on the compressive bar  $\phi 8$  and tensile reinforcement, inside of the middle cross section. All measuring devices (LVDTs and SGs) together with the load cell were connected to HBM 8 channel spider to record the data. From here, data were forwarded to computer using a specific software program, where they are processed and stored in a text file.

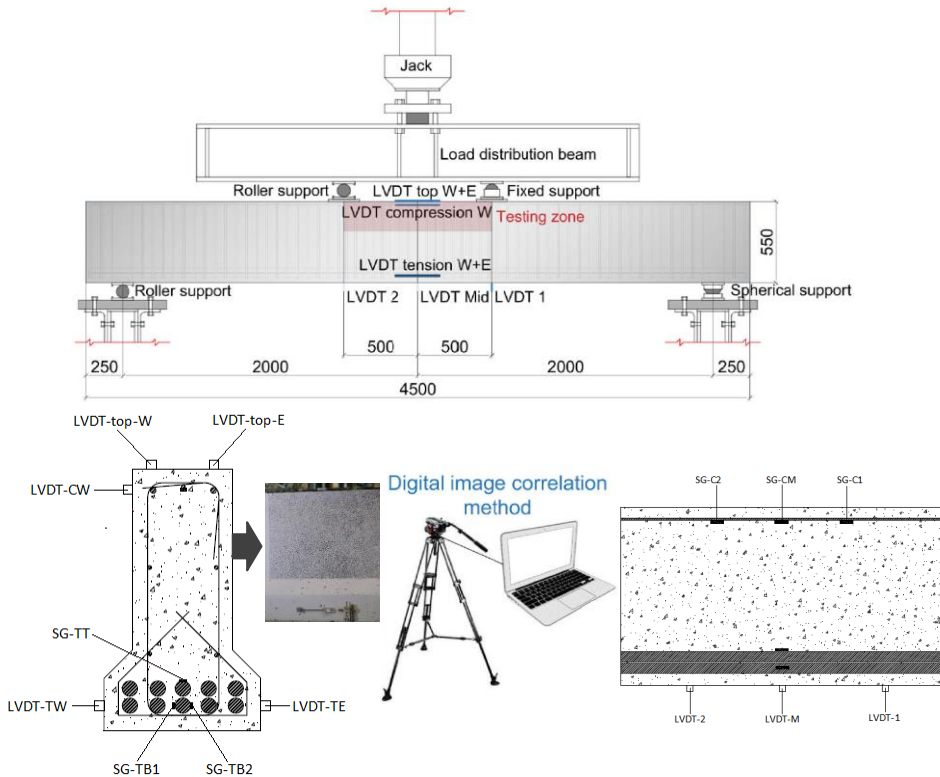


Fig. 2 Top of the figure show experimental set-up of the beam test. At the bottom of the figure, there is sketch of cross section at the middle of testing area with location of each measuring devices. Dimensions are in [mm].

The load was applied step-wise, with load increments of 100 kN up to 70% of calculated capacity. The load increments were then reduced to 50 kN until failure. The rest periods at each load level were three minutes and mainly used to draw the crack progression with dark pen and taking of photos.

The tests were displacement controlled with a loading rate 1-1.2 mm/minute, thus, the deflection measurements were carried out as a control during all tests.

### 3. Experimental results

#### 3.1 Results for small specimens

Small specimens were tested after 28 days for determination of compressive strength, tensile strength and Young's modulus. Small beams for fracture energy were tested after 71 days. A brief summary of the small-scale test results is given in Table 3. Concrete class measured from small samples was LC65 and which represents a high strength lightweight concrete. The compressive failures of cubes and cylinders were very explosive which is typical for high strength and lightweight concrete.

Table 3 Mechanical properties LWAC 65

Saturated density	$\rho_{cs} = 2013 \text{ kg/m}^3$
Oven dry density	$\rho_{cv} = 1834 \text{ kg/m}^3$
Compression cube after 7 days	$f_{icm,7} = 56.7 \text{ N/mm}^2$
Compression cube after 28 days	$f_{icm,28} = 74.2 \text{ N/mm}^2$
Compression cylinder	$f_{icm} = 65,1 \text{ N/mm}^2$
Tensile strength	$f_{lctm} = 4.03 \text{ N/mm}^2$
Modulus of elasticity	$E_{lcm} = 24175 \text{ N/mm}^2$
Fracture energy	$G_F = 70.5 \text{ Nm/m}^2$
Characteristic length	$l_{ch} = 104 \text{ mm}$

#### 3.2 Capacity of the beams

Table 4 shows the results of the tested beams. The beams were tested 37 days (beam 1), 50 days (beam 2 and 3), 55 days (beam 4), 57 days (beam 5) and 59 days (beam 6) after casting. Each beam experienced spalling of the concrete cover in compression between the loading points. Spalling defines the first load peak in the load-deflection curves. The load decreased at this stage for some minutes, before the applied load again increased. The load, then, continued to increase until the concrete cover in the web started to spall. This defines as a second load peak and is a more smooth peak. The second spalling resulted in a larger drop in the load bearing capacity and deformations increased fast. Any attempt to increase load after second peak was not possible and residual capacity of the beam decreased until the final failure.

Table 4 presents the obtained results: the force when the first bending crack occurred ( $P_{fcr}$ ), force of first shear crack ( $P_{cr}$ ), force corresponding to first peak load ( $P_1$ ), force corresponding to second peak load ( $P_2$ ) and force corresponding to the failure load ( $P_u$ ). The table also gives average strains ( $\epsilon_c$ ) recorded by two LVDTs placed in the compression zone. Value of recorded maximum strains correspond to first peak load level. The average tension strain ( $\epsilon_t$ ) represents the two LVDTs placed on both bottom beam sides in the tensile zone. The bending capacity ( $P_{calc}$ ) for all the tested beams was calculated according to Eurocode 2 and Norwegian standard [6], [7]. When calculating the capacity of the beams compressive strength, tensile strength, E-modulus and strains in a concrete were multiplied by a reduction factors  $\eta_1$ ,  $\eta_E$  and those values are respectively 0.746 and 0.918.

Table 4 Results from beam testing

Beam Identification	$f_{lc,cube}$ [MPa]	$P_{calc}$ [kN]	$P_{fcr}$ [kN]	$P_{cr}$ [kN]	$P_1$ [kN]	$P_2$ [kN]	$P_u/P_{calc}$ [kN]	$\epsilon_c$ [‰]	$\epsilon_t$ [‰]
LWAC65_20_0	75.4	729	53	318	724	-	0.99	3.70	-
LWAC65_20_200	78.3	729	54	350	645	629.4	0.88	3.77	2.04
LWAC65_20_60	78.3	729	78	319	707	686.5	0.97	3.74	2.41
LWAC65_20_100	79.4	729	69	324	700	-	0.96	3.75	2.08
LWAC65_40_100	79.4	726	64	339	663	588.9	0.91	3.61	2.17
LWAC65_40_200*	79.4	800	64	250	750	652.9	0.94	3.40	2.35

#### 4. Discussion

For all the tested beams failure occurred when the compression zone between the loading points started to crack. This type of failure defines a compressive failure in the bending moment zone. Cracking of the compression zone was different for each beam depending on the test parameters: stirrup spacing, size of concrete cover and amount of the compressive reinforcement.

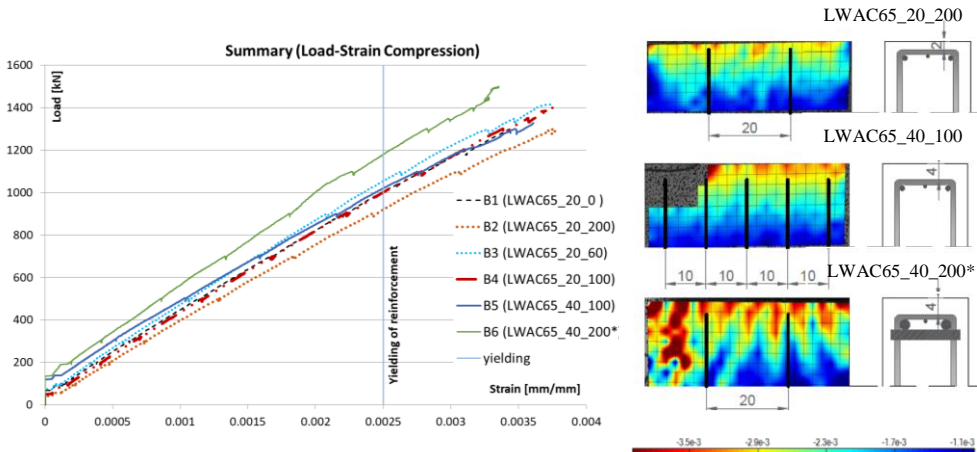


Fig. 3 Left side of the figure shows graph where is plotted average strain in compression at the mid-span versus total applied load. At the right side are plotted strain fields recorded by digital image correlation method for the first peak load level.

The first bending cracks observed in the constant moment region on the tension side, was at load levels from 25 til 53 kN. First cracking depends on the stirrups density in testing area. Since beam without any stirrups in testing area did not have any confinement this beam cracked for lowest load level. As the load increased, new bending cracks propagated symmetrically until they reached the top of the beam flange. Development of bending cracks slowed down when shear cracks appeared. The first shear cracks appeared in the middle of the shear zone, between the neutral axis and the beam flange. Additional loading lead to further crack propagation of both bending and shear area. Crack propagation for certain load steps are very similar for all the tested beams. From Table 4 it is obvious that beams which contain the stiff compressive reinforcement and most stirrups in testing area was able to sustain the largest load before spalling of the concrete cover. From Fig. 3 it can be seen that the compressive longitudinal reinforcement yielded for the largest load level. Beams with large stirrup spacing and small concrete cover showed the fastest spoiling and increase in crack propagation. When

the applied load reached first peak, the cross section for all the beams was reduced due to the spalling of the top concrete cover with load automatically decreasing. It is obvious that beams with large concrete cover has higher drop in capacity and the second peak load level was lower. In finale face, spoiling of the web occurred and load drop very fast, while deformations increased, see Fig. 3. Beams with more dense stirrups can sustain more loading after first peak and they showed behaviour that is more ductile. In beam without stirrups in testing area and with low concrete cover second peak load was not registered. The beam failed immediately after first peak load level. Since all the beams were over-reinforced, tensile reinforcement did not yield.

From Fig. 3 it can be concluded that strains recorded by measuring devices LVDTs and DIC was the same. Ultimate compressive strain registered in the beams was in range 3.4-3.8%. By using DIC, detailed strain fields of the observed compressive zones have been recorded, and DIC was able to measure strain after spoiling of the top concrete cover together with LVDTs. From the detailed strain field it can be seen localisation of the largest strains in areas prior to failure. It is also visible that strains distribution followed reinforcement detailing. In a beam with the largest compressive reinforcement, strains were deeper. The same holds for concrete cover, with larger cover, large strains are deeper and spalling of concrete follows reinforcement layout. In addition, it is visible that reinforcement layout influence the most crack development. Cracks were formed between stirrups. Having in mind that EC2 [6] has special rules for LWAC, which are reduction factors applied to regular design criteria, the results in this study indicate that EC2 underestimates LWAC. Recorded maximum strains in the tested beams were for 30-50 % larger than the standard allowed maximum strain ( $\epsilon_{cu2}=2.52\%$ ), for this type of concrete.

In general, observed cracking in all the tested beams were very similar as could be expected in normal weight concrete beams, see Fig. 4.



Fig. 4 Figure of the failure for beam 4 (LWAC65\_20\_100).

## 5. Conclusions

For all tested beams in this research cracking were similar. All the beams showed ductile behaviour since they were able to increase loading after formation of shear cracks. Cracking of the testing area depend on the test parameters varied in the experiment. Beams with dense stirrup spacing showed small, shallow cracks and spoiling were smallest. In beams where cover was deeper spoiling and cracking were larger. The beam containing the largest compressive reinforcement resisted the largest load. Beam without stirrups in testing area failed at first peak load level. Measuring devices were able to capture the ultimate compressive strain in LWAC beams.

In general, the characteristics of LWAC depend on the type of lightweight aggregate. EC2 does not differentiate between types of aggregate used in LWAC. From the experimental results, it can be seen that EC2 underestimates ultimate strain level with 30-50%. This study with LWAC indicates bending behaviour similar to NDC. From the experimental program, it can be concluded that by proper reinforcement detailing it is possible to achieve ductile response of lightweight concrete structures. The response in the tested beams were only a small reduction in load capacity after reaching a peak load, followed by an increased deformation. By being able to document a larger ultimate compressive strain in LWAC beams, an increased use of LWAC in structural applications are possible. Further investigations of LWAC as a structural material should therefore continued.

## Acknowledgements

The work presented in this paper is part of an ongoing PhD study in the DACS project (Durable Advanced Concrete Solutions). The DACS partners are Kværner AS (project owner), Norwegian Research Council, Axion AS (Stalite), AF Gruppen Norge AS, Concrete Structures AS, Mapei AS, Multiconsult AS, NorBetong AS, Norcem AS, NPRA (Statens vegvesen), Norwegian University of Science and Technology (NTNU), SINTEF Byggeforsk, Skanska Norge AS, Unicon AS and Veidekke Entreprenør AS. The first author would like to express her outmost gratitude to the supervisors and all the project partners for contributions and making this PhD study possible. In addition, special gratitude goes to master students Simon André Petersen, Henrik Nesje Johannesen, Jonas Andås Belayachi and Khaled Bastami for help during production and testing in this study.

## References

- [1] Satish, C., and Leif B. 2002. *Lightweight Aggregate Concrete*. USA. Noyes publications-Wiliam Andrew Publishing.
- [2] ACI Committee 213. (ACI213R-03). *Guide for structural lightweight aggregate concrete*. 2003. Farmington Hills (MI, United States): American Concrete Institute.
- [3] Melby, K. 2000. "Use of high strength LWAC in Norwegian bridges." Paper presented at the International symposium on structural lightweight aggregate concrete, Norwegian Concrete Association, Kristiansand, Norway, June 18-22.
- [4] Castrodale, R. W., Zivkovic, J. and Valum, R. 2017. "Material Properties of High Performance Structural Lightweight Concrete." Paper presented at the Eleventh High Performance Concrete (11<sup>th</sup> HPC) & the Second Concrete Innovation Conference (2<sup>nd</sup> CIC) Tromsø, Norway, March 6-8.
- [5] Haug, A. K., Fjeld, S. 1996. "A floating concrete platform hull made of lightweight aggregate concrete." *Engineering Structures*, Vol. 18, No. 11, November, pp 831-836.
- [6] EN-1992-1-1. 2004. "Eurocode 2, Design of concrete structures – Part 1-1: General rules and rules for buildings". Brussels, Belgium: CEN European Committee for Standardization.
- [7] NS-EN 1992-1-1:2004+NA: 2008. 2008. "Eurocode 2: Design of concrete structures – General rules and rules for buildings", Standard Norway.
- [8] RILEM TC 148-SSC: Strain softening of concrete - Test methods for compressive softening, Test method for measurement of the strain-softening behavior of concrete under uniaxial compression. 2000. *Materials and Structures*, Vol. 33, July, pp 347-351.
- [9] Nedrelid, H. 2012. "Towards a better understanding of the ultimate behaviour of lightweight aggregate concrete in compression and bending." PhD diss., Norwegian University of Science and Technology.
- [10] Øverli, J. A., 2017. "Towards a better understanding of the ultimate behaviour of LWAC in compression and bending." *Engineering Structures*, Vol. 151, pp 821–838.
- [11] Fayyada, T.M. and Leesb, J.M. 2014. "Application of Digital Image Correlation to Reinforced Concrete Fracture." *Procedia Materials Science* Vol. 3, 20<sup>th</sup> European Conference on Fracture (ECF20), pp 1585 – 1590.
- [12] McCormick, N. and J. Lord. 2012. "Digital Image Correlation for Structural Measurements." *Proceedings of the Institution of Civil Engineers - Civil Engineering*, Vol. 165, Issue 4, November, pp 185-190.
- [13] Carolina Stalite Company. 2009. "Benefits of using Stalite." Accessed October 21. <http://www.stalite.com/why-use-stalite.php?cat=138.html>.
- [14] Kotsovos M.D., 1983. "Effect of testing techniques on the post-ultimate behaviour of concrete in compression." *Materials and Structures*, Vol. 16, Issue 1, pp 3–12.
- [15] NS 3576-3:2012. 2012. "Armeringsstål - mål og egenskaper - del 3: Kamstål B500NC.", Standard Norge.